

# Tuning Structural and Electronic Properties of Phosphorene with Vacancies

*N. Pantha, B. Chauhan, P. Sharma and N. P. Adhikari*

**Journal of Nepal Physical Society**

*Volume 6, Issue 1, June 2020*

*ISSN: 2392-473X (Print), 2738-9537 (Online)*

**Editors:**

Dr. Binod Adhikari

Dr. Manoj Kumar Yadav

Mr. Kiran Pudasainee

*JNPS*, 6 (1), 7-15 (2020)

DOI: <http://doi.org/10.3126/jnphysoc.v6i1.30428>

**Published by:**

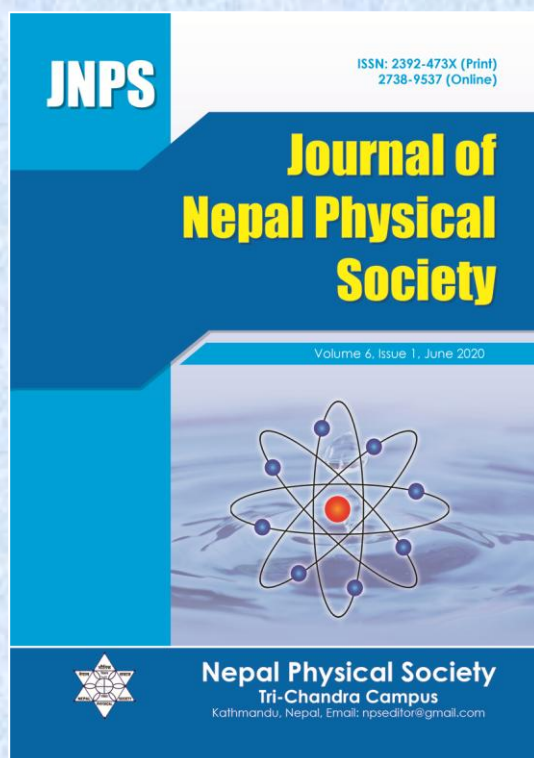
**Nepal Physical Society**

P.O. Box: 2934

Tri-Chandra Campus

Kathmandu, Nepal

Email: [npseditor@gmail.com](mailto:npseditor@gmail.com)





# Tuning Structural and Electronic Properties of Phosphorene with Vacancies

N. Pantha, B. Chauhan, P. Sharma and N. P. Adhikari\*

Central Department of Physics, Tribhuvan University, Kirtipur, Kathmandu, Nepal

\*Corresponding Email: npadhikari@gmail.com

**Received:** 15 Mar., 2020; **Revised:** 18 May, 2020; **Accepted:** 25 June, 2020

## Abstract

Two dimensional materials show multiple applications including in semiconductor devices and gaseous storage. We have carried out First-Principles calculations to study the geometrical structures, stability and electronic/magnetic properties of pristine as well as double vacancy phosphorene. Calculations are based on Density Functional Theory (DFT) taking an account of van der Waals (vdW) interaction in the DFT-D2 approach within Generalized Gradient Approximation (GGA). Modeling and simulation have been performed with Quantum ESPRESSO (QE) codes. The supercell of  $4 \times 4$  structure, whose building block is an orthogonal unit cell with four phosphorous atoms, is used to model the samples. Based on the stability of defected single layer phosphorene, a couple of structures (DV(5|8|5)-1 and DV(5|8|5)-2) have been considered to calculate their formation energy, band structure and other properties. Formation energy values find the former structure (DV(5|8|5)-1) more favorable to create than the later one. A band gap of 0.86eV for pristine phosphorene, an excellent agreement with the experiment, validates the results of present calculations. The phosphorene with double vacancy, however, shows significant changes in electronic bands with reference to the pristine one. The band gap for DV(5|8|5)-1 and DV(5|8|5)-2 systems are found to be 1.01eV and 0.1 eV respectively. No magnetic moment in both the pure and defected (double vacancy) phosphorene monolayer approves that only the vacancies are not enough to induce magnetic properties in phosphorene.

**Keywords:** Band structure, Formation energy, Phosphorene, Vacancies.

## 1. INTRODUCTION

The atomic planes of the two-dimensional crystals are weakly held to each other by van der Waals (vdW) forces so that they can be easily peeled off, leaving no dangling bonds [1]. Unlike bulk structure, they possess some specific features like: intrinsic high mobility, thickness proportional band gap, high degree of mechanical stability, high surface to volume ratio [2] and offer a better platform for various opto-electronic applications that stems for their unique electrical, mechanical, and optical properties [3].

Graphene, a one atom thick crystalline allotrope of carbon, could be one of the obvious choices from two dimensional materials due to its high strength, and electrical/thermal conductivity. In spite of such wonderful properties, zero band gap of graphene limits its use in electrical circuits [1]. Two-dimensional transition metal dichalcogenides

(TMDCs) were introduced to overcome this limitation with tunable band gap (depending upon the number of layers) [4, 5]. However, the carrier mobility of these materials were merely tens of  $\text{cm}^2\text{V}^{-1}\text{s}^{-1}$  which is much lower than that of the graphene. In this context, phosphorene has aroused a considerable attention due to its high carrier mobility and appreciable band gap which makes it different from graphene and other two dimensional materials. The monolayer of phosphorene consists of mobility (hole dominant) of order  $1000 \text{ cm}^2\text{V}^{-1}\text{s}^{-1}$  [6] and electronic band gap in the order of 0.9 eV [7]. It is an intrinsic p-type semiconductor whose band gap (direct band gap) can be modified on changing the number of layers [6]. It can also exhibit the superconductivity above 10 K with suitable doping [8] and has tunable work function that increases with the thickness of layers.

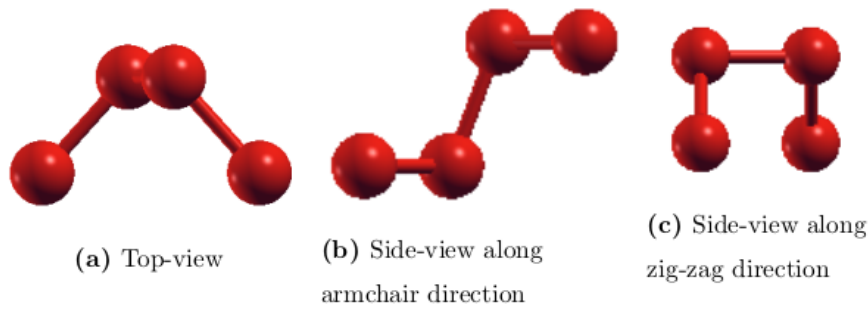


**Fig. 1:** Top view and side view of phosphorene unit cell (containing four phosphorous atoms).

Phosphorene is a two-dimensional allotrope of phosphorous which was discovered in 2014 by liquid exfoliation method [9]. At room temperature black phosphorus is the most stable allotrope of phosphorus which was synthesized from white phosphorous under high pressure and temperature [10, 11]. Phosphorene consists of honeycomb lattice and the single layer of it exhibits a quadrangular pyramid structure (Fig. 1). The lattice parameters (cell size and atomic positions) of the structure are available in already reported studies [12] and also discussed in later section. Since phosphorene consists of non magnetic phosphorous atoms, it has no spin polarized states. Among two different structural edge terminations (Fig. 2), zigzag nanoribbons possess metallic bands where as armchair nanoribbons are semiconductors. Because of its unique features, various applications like in gas sensor, Li-ion battery, energy storage device and solar cells have been proposed [13].

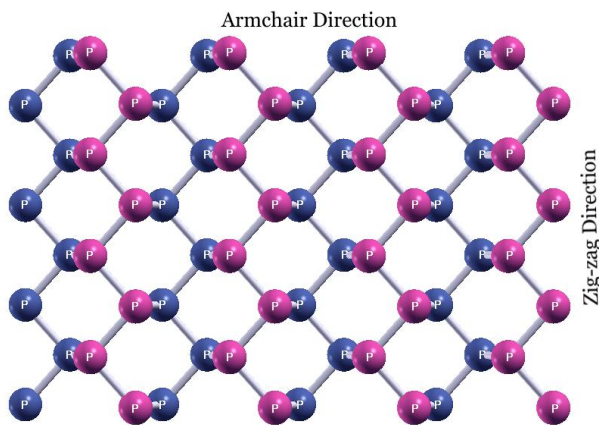


**Fig. 2:** Monolayer phosphorene shows armchair and zigzag directions.

Crystalline solid possesses a periodic structure where the position of molecules or atoms occurs in

regular fashion. However there is always a possibility of missing/lacking or the presence of foreign atoms/ions in an ideal crystal structure, called defects. Defects are essential for a crystal to be in equilibrium. One can find various types of defects; like Stone-Wales (SW) defect, Single vacancy (SV), and double vacancy (DV) defects in low dimensional materials [14-16]. Most of them are easy to distinguish each other and correlate with their atomic structures with simulated scanning tunneling microscopy (STM) images. Defects are always crucial to change the material properties in two dimensional systems. Vacancy can induce magnetism in case of graphene [17, 18] but only the vacancy cannot induce it in MoS<sub>2</sub> [19, 20]. In case of phosphorene, neither monovacancy nor strain alone can create magnetism, however, the interplay between monovacancy and the strain is able to induce effective magnetization in phosphorene [21]. In spite of a number of studies, many properties of double vacancy created (defected) phosphorene monolayers are yet to be resolved.

In this paper, we apply spin polarized density functional theory (DFT) method to explore the effect of double vacancy (two atoms are removed from their normal position) in monolayer phosphorene with two possible structures. We analyze the geometrical, electronic, and magnetic properties of defected phosphorene comparing to that of pure phosphorene. After this introduction part, we describe the computational method, results and discussion, and conclusions in order.

## 2. COMPUTATIONAL DETAILS

Structural, electronic and magnetic properties of double vacancy phosphorene with reference to pristine one have been studied by using density functional theory based approximations [22, 23] with vdW interactions in DFT-D2 approach [24]. We have used Quantum-Espresso (version 5.0.1)

codes to model the systems under consideration. The electronic exchange and correlation effects have been accounted by using generalized gradient approximation (GGA) of Perdew, Burke and Ernzerhof (PBE) form [25]. In addition to this, Rappe-Rabe-Kaxiras-Joannopoulos (RRKJ) ultrasoft pseudopotential (USSP) was used to substitute the effects of non-valance electrons and the nucleus with an effective potential [26, 27].

In order to get optimized structure of supercells, we relaxed the system using Boroyden-Fletcher-Goldforb-Shanno (BFGS) [28] method unless the difference in energy between the two consecutive 'scf' is  $10^{-6}$  Ry and difference in each component of force acting is less than  $10^{-3}$  Ry/Bohr. Monkhorst-Pack scheme was used to sample the Brillouin zone for self consistent total energy calculations [29]. We set the 'Marzari-Vanderbilt' (m-v) smearing [30] with small width of 0.002 Ry to run the scf calculations. Further 'david' diagonalization method with a mixing factor 0.6 was used for self consistency.

There are five valence electrons in a single phosphorous atom. Among them three electrons form covalent bonds with other three phosphorous atoms resulting a lone pair of electrons. Phosphorene consists of honeycomb structure and the single layer of it exhibits a quadrangular pyramid structure because of the covalent bond between three phosphorous atoms with other [31]. The atomic positions, interatomic distances and the lattice parameters of the structure have been fixed with the help of convergence tests (shown in Fig. 3 and Table 1). The interlayer separation has been set  $20 \text{ \AA}$  ( $c = 20.0 \text{ \AA}$ ) along perpendicular direction to the crystal plane to avoid the interaction between the successive layers. The kinetic energy cutoff for plane waves (38 Ry) and also the number of k-points along x and y directions have been fixed ( $k_x, k_y = 24$ ) following the procedure of

convergence tests. The number of k-points along z-direction, however, is set to unity because of its monolayer structure.

Once a stable/relaxed unit cell of phosphorene is constructed with appropriate lattice parameters, supercells of  $2 \times 2$ ,  $3 \times 3$  and  $4 \times 4$  can be generated by translating the unit cell along X- and Y- directions. To minimize the interaction between the periodic defected (double vacancy) phosphorene units, we have used  $4 \times 4$  supercell for further calculations. Following the process of atomic optimization, we then calculated the band structure, formation energy, density of states and partial density of states of  $4 \times 4$  pristine supercell and vacancy created  $4 \times 4$  supercells. Band structure calculations were performed with 100 k-points extracted along the specific direction of irreducible Brillouin zone.

### 3. RESULTS AND DISCUSSION

We discuss the geometrical structure, formation energy, and band structure of the pure and double vacancy phosphorene sheet in this section.

#### 3.1. Geometrical structure and formation energy

##### 3.1.1. Pure phosphorene

Phosphorene consist of honeycomb lattice and the single layer of it exhibits a quadrangular pyramid structure. The lattice parameters and the atomic arrangement of phosphorene unit cell are shown in Fig. 3 and Table 1 where two atoms are in plane of the layer at an angle of  $96.31^\circ$  from each other ( $\theta_1=96.31^\circ$ ) and the third atom is between the layers at an angle of  $103.57^\circ$  ( $\theta_2=103.57^\circ$ ). The bond length between two consecutive phosphorous atoms lying in same plane is  $2.22 \text{ \AA}$  ( $d_1 = 2.22 \text{ \AA}$ ) and in different planes is  $2.25 \text{ \AA}$  ( $d_2 = 2.25 \text{ \AA}$ ). The lattice parameters have been found as  $\mathbf{a} = 4.56 \text{ \AA}$  (along armchair direction),  $\mathbf{b} = 3.31 \text{ \AA}$  (along zigzag direction), which are in good agreement with the theoretical calculations [6] and an experiment [12].

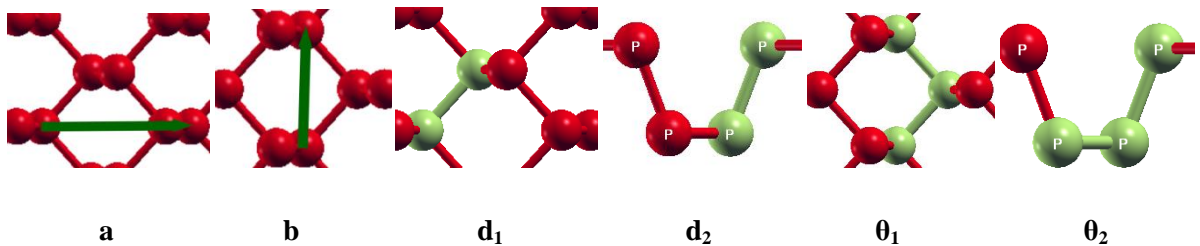


**Fig. 3:** Lattice parameters, bond lengths, and bond angles of unit cell of phosphorene. Light green color denotes specified parameters.



**Table 1: Calculated values of lattice constants, bond angles and bond lengths and those extracted from experimental and theoretical papers. The parameters under comparisons are illustrated in Fig.[3].**

	<b>a</b> (Å)	<b>b</b> (Å)	<b>d<sub>1</sub></b> (Å)	<b>d<sub>2</sub></b> (Å)	<b>θ<sub>1</sub></b>	<b>θ<sub>2</sub></b>
Observed (monolayer)	4.56	3.31	2.22	2.25	96.31°	103.57°
Experimental (bulk) [12]	4.38	3.31	2.22	2.28	96.34°	102.09°
DFT-PBE [6]	4.57	3.30	2.22	2.26	95.98°	103.59°

Monolayer phosphorene of size 4×4 supercell consists of 64 phosphorous atoms with lengths and breaths in x and y- directions as **a** = 18.24 Å and **b** = 13.24 Å. As atoms are arranged in two different planes, different colors are used for respective planes, for upper plane and lower planes (Fig. 2). The strength of binding an individual atom in phosphorene sheet can be calculated by binding energy per atom. We first calculate the total energy required to assemble atoms in the phosphorene sheet by using equation (1) and then divide by the number of atoms (*N*) to find binding energy per atom.

$$\Delta E = N \times E_{pi} - E_{phosphorene} \dots\dots\dots(1)$$

Here  $\Delta E$  is the binding energy (B.E), *N* is the total number of phosphorus atoms,  $E_{pi}$  is the ground state energy of a single isolated phosphorus atom, and  $E_{phosphorene}$  is the ground state energy of phosphorene supercell under consideration. For a stable system (bound system) the B.E per atom values ( $\Delta E$ ) should always be positive. Present calculations find binding energy per atom as 3.60 eV which is large enough for the stability of monolayer phosphorene.

### 3.1.2. Defected phosphorene with vacancies

Defects are imperfection in regular crystal structure which is inevitable. We consider double vacancy (taking out two phosphorous atoms from their normal position) in relaxed phosphorene monolayer to study change in structural, electronic and magnetic properties. Among the various relative positions from where the atoms can be picked out, we have considered two types of double vacancy in a 4×4 supercell. They are: (i) neighboring atoms in the same plane (**P35** and **P38** atoms of Fig. 4) and (ii) two neighboring atoms located in two different planes (**P31** and **P35** of Fig. 4). When the structures

are allowed to get full relaxation after removing particular atoms, they form different bonding/symmetry-rings comparing to that of the pristine one. Both the defected/reconstructed phosphorenes form two pentagons and one octagon near to the defect sites in addition to the regular hexagons (Fig. 5). Based on new symmetry they form, the structures are then named as DV(5|8|5)-1 and DV(5|8|5)-2 respectively.

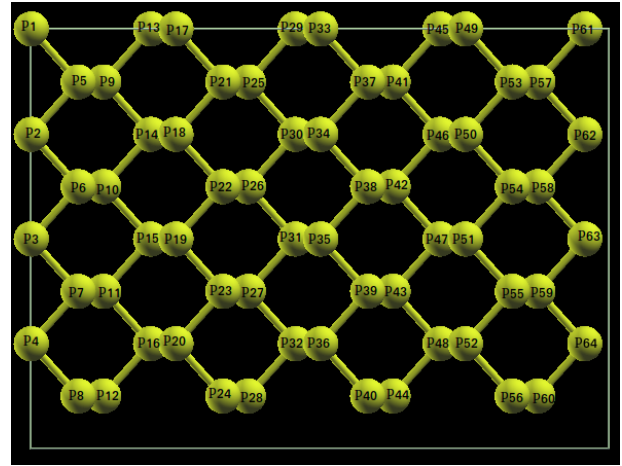


**Fig. 4:** Site numbers of phosphorous atoms for the purpose of creating vacancies at particular positions.

To study the effect on geometrical structure of defects, we measured bond lengths between the phosphorous atoms of more favorable structure (DV(5|8|5)-1, will be discussed later) in the vicinity of impurity sites and compared with values with the corresponding atoms in pure phosphorene (Table 2). In case of pure phosphorene, phosphorous atoms arrange covalent bonding with planar ( $d_1 = 2.22$  Å) and interplanar ( $d_2 = 2.25$  Å) closest neighbors (tolerance 0.01 Å). The larger distance (3.40 Å) in between **P34-P42** and **P39-P31** is due to their non-neighboring positions in pure system.

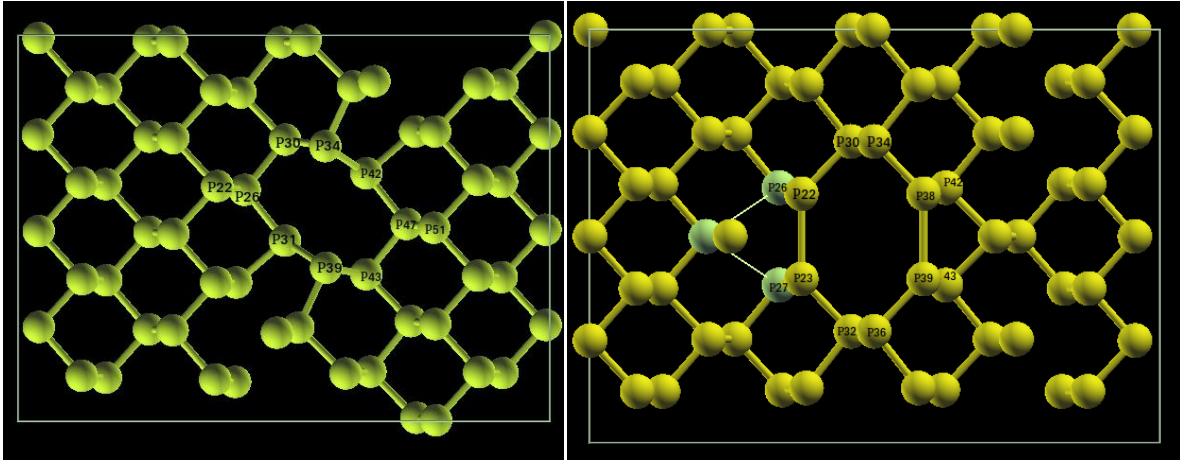


**Fig. 5:** Two different divacancy phosphorene structures [DV(5|8|5)-1 and DV(5|8|5)-2] under consideration in the present work.

After getting relaxation of the defected structures, the bond length in between the nearest neighbors may change (Table 2). Some of the atoms which were not the nearest neighbors in pure system become the nearest neighbors due to removal of nearby atoms. There is almost no change in bond length between the atoms in same plane (variation in the order of error bar  $\sim 0.01$  Å) comparing to that of the atoms in different planes (variation up to  $0.03$  Å). There is, in

general, decrease in bond length due to increase in number of atoms in newly formed octahedral ring. Atoms nearby missing atoms, however, show a significant contraction in bond length comparing to that of in pure system (before relaxation in defected system). The distance between **P34** to **P42** for an example reduced to  $2.40$  Å from  $3.52$  Å. This change in distance can be understood in terms of rearrangement of atomic bonding nearby missing atoms.

**Table 2:** Interatomic distance between the neighboring atoms close to vacancy sites for DV(5|6|5)-1 and pristine supercell.

S.N.	Bond length DV(5 8 5)-1	Value of bond length (Å)	Corresponding value in pristine phosphorene (Å)
1	P22-P26	2.23	2.25
2	P26-P30	2.22	2.22
3	P30-P34	2.23	2.26
4	P34-P42	2.40	3.52
5	P42-P47	2.23	2.22
6	P47-P43	2.22	2.22
7	P43-P39	2.25	2.25
8	P39-P31	2.40	3.52
9	P31-P26	2.23	2.22
10	P47-P51	2.24	2.26

To study the effect of vacancies on the stability of monolayer phosphorene, we carried out the calculations of formation energy (required energy for the formation of defect/s) for both the defected phosphorene systems (DV(5|8|5)-1 and DV(5|8|5)-2). The formula used for the calculation is

$$E_{form} = E_{defect} - E_{ideal} + n \times E_{pi} \dots \dots \dots (2)$$

where,  $E_{ideal}$  is the total energy of pristine phosphorene monolayer,  $E_{defect}$  is the total energy of defected phosphorene supercell,  $E_{pi}$  is the energy of an isolated phosphorous atom, and  $n$  is the

number of missing atoms as vacancy in the supercell ( $n = 2$  for divacancy). The positive value

of formation energy means that the energy is absorbed while creating defects.

**Table 3: Vacancy formation energy values from the present calculations and previously reported results.**

S.N.	Structure (DV)	$E_{form}$ (eV) Our calculated results	$E_{form}$ (eV) Reported results [32]
1	DV(5 8 5)-1	2.743	1.906
2	DV(5 8 5)-2	5.301	3.041

Table 3 shows the results of the formation energy for two types of divacancy calculated using equation (2). From the table we can see that the formation energy of DV(5|8|5)-1 is almost half (2.743 eV) than that of the DV(5|8|5)-2 (5.301 eV) making it most favorable structure in case of divacancy. The results from the present calculations fall in the same order of magnitudes with reference to the values available in previous studies [32]. The discrepancy in between the studies can be understood in terms of different pseudopotentials and size of the supercells.

### 3.2. Electronic properties

We discuss the band structure calculations and density of states of pure as well as defected phosphorene in this section.

#### 3.2.1. Pure phosphorene

The discrete energy levels of individual atoms/molecules change into a continuum energy levels in a solid due to a large number of nearby energy orbital, known as a band [27]. Among the number of energy bands of a system/solid, outer energy bands are important to study their electronic structure. Based on the nature of energy difference between the valence band (highest occupied level) and the conduction band (lowest unoccupied level), solids can be classified into insulators, semiconductors and conductors. In case of insulators and semiconductors, no electron orbital exists in between valence band and conduction band. These energy bands, however, overlap in metals due to two partially filled bands.

The smallest volume enclosed by the planes that are perpendicular bisectors of the reciprocal lattice vectors drawn from the origin is known as first Brillouin zone. Fig. 6 illustrates the first Brillouin zone of orthorhombic lattice with high symmetry points. Since interlayer separation along z-axis has been made very high to neglect the interlayer interaction, the band structure

calculations were modeled along the high symmetry points on the edge of irreducible Brillouin zone. With 100 k-point grids, the sampling path of  $\Gamma$ -X-S- $\Gamma$ -Y-S has been used in the present work.

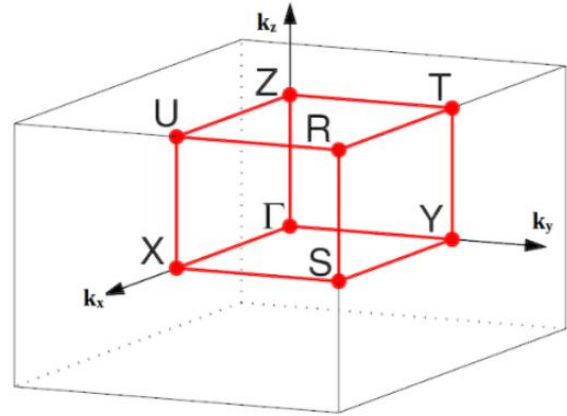


**Fig. 6:** The first Brillouin zone (Bz) of orthorhombic lattice showing high symmetry points. Small volume, enclosed by bold (red) margins, which is one-eighth of volume of first BZ represents irreducible Brillouin zone.

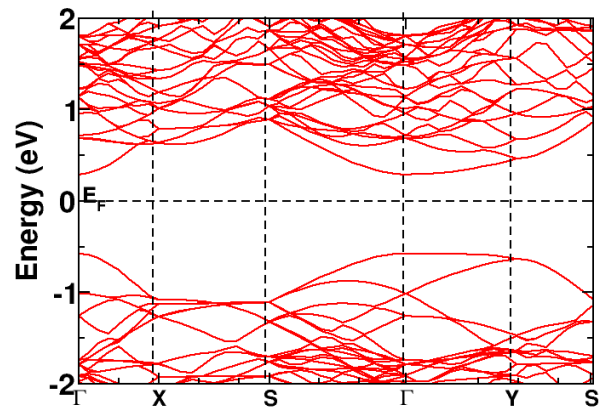


**Fig. 7:** Band structure of pristine phosphorene shows the direct band gap at  $\Gamma$  point.

Fig. 7 shows the band structure of pristine phosphorene from the present calculations. The

structure from the present calculations has a good agreement with the previous study [7] in terms of nature (direct band gap) and the value of the band gap. Both the results show the bottom of the conduction band and top of the valence band lie at  $\Gamma$  point. We have found the magnitude of band gap as 0.86 eV which is very near to the reference (0.9 eV) [7]. In the reference, the authors have used DFT-HSE06 level of approximations which describes the small difference between these two results.

A close view of Fig. 7 shows that the conduction band minima (CBM) lies 0.28 eV above the Fermi level and valence band maxima (VBM) 0.58 eV below it resulting the band gap of 0.86 eV. The higher number of band lines (orbitals) in our calculations is due to the fact that we have

considered  $4 \times 4$  supercell containing 64 phosphorous atoms for simulation whereas the unit cell in reference contains only 4 phosphorous atoms. The band structure calculations of phosphorene approves that the material is semiconductor in monolayer structure.

### 3.3. Defected phosphorene

Two atoms (from different positions) have been removed to create defects in monolayer phosphorene (Fig. 8). They are named as DV(5|8|5)-1/DV(5|8|5)-2 and their structure are described above. Here we present, discuss and compare the band structure of double vacancy created phosphorene with pristine phosphorene.

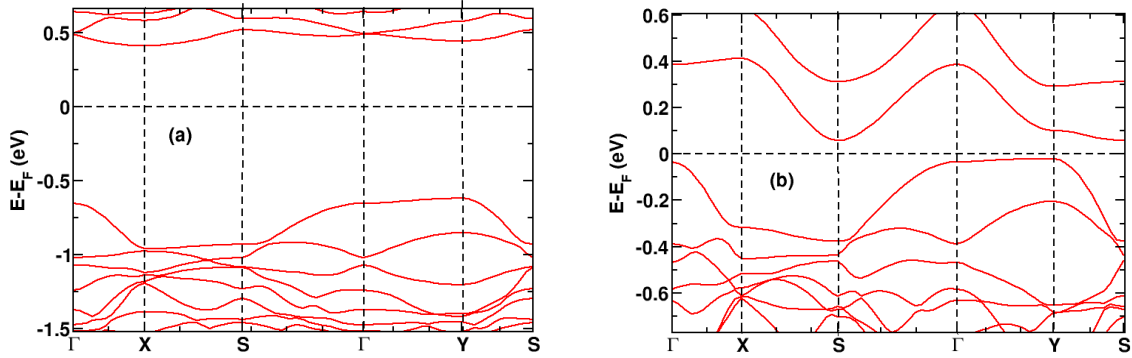


**Fig. 8:** Band structure calculations of defected phosphorene for (a) DV(5|8|5)-1 and (b) DV(5|8|5)-2 type of vacancies.

Fig. 8 shows band structure calculations for double vacancy phosphorene (DV(5|8|5)-1 and DV(5|8|5)-2). Since some of the atoms are removed from their normal positions in periodic lattice, there is the formation of unsaturated bonds and new type of interaction exists specially in between atoms nearby vacancy sites. This new type of geometrical structure changes its electronic structure/distribution over the sheet. Hence the nature and position of electronic orbitals keep changing. Fig. 8(a) represents the band structure of DV(5|8|5)-1 structure, where it keeps direct nature of band gap intact, however, the magnitude and position are changed. The band gap increases from 0.86 eV (in case of pristine phosphorene) to 1.01 eV and the position of minimum energy gap shifts from  $\Gamma$  point to Y point of the Brillouin zone. On the other hand, Fig. 8(b) represents the band structure of DV(5|8|5)-2 structure where the direct band gap (in pristine case) changes to indirect one. The minimum of conduction band and maximum of

valence band are found at S point and Y point respectively. The band gap decreases from 0.86 eV (in pristine phosphorene) to 0.1 eV. It is clear that some extra orbitals appear near to the Fermi level. Hence the tuning of band gap due to double vacancy in phosphorene seems to be position dependent.

Density of States (DOS) gives the number of quantum states per unit energy range. It indicates how densely the quantum states are packed in a system or how many orbitals per unit energy range at particular energy level are available to be occupied. With the help of DOS we have analyzed the distribution of energy states (Figures are not shown here) as a function of energy and verified the energy gap near to Fermi level which are already discussed in band structure. We know that the asymmetry, if any, in density of states between up spin and down spin gives the magnetic property of materials. Present calculations find DOS for all the tested



geometries (pure phosphorene, DV(5|8|5)-1 and DV(5|8|5)-2) symmetric. Hence the systems are non-magnetic and conclude that only the vacancies cannot create magnetic behavior in phosphorene. This finding comes in agreement with the previous study where neither the vacancy (monovacancy) nor the strain could create magnetism [33]. The partial density of states (PDOS) calculations of the systems finds that 3p-orbitals of phosphorous atoms give significant contribution near by the Fermi level. Also in case of DV(5|8|5)-2, energy gap is hardly seen near to Fermi-level. This implies that small band gap (0.1 eV) for the structure could fall in error bar of the calculations and further verification might be required.

#### 4. CONCLUSIONS

Density functional theory based first-principles calculations have been performed to study the geometrical stability and electronic properties of pure and defected (double vacancy) phosphorene. The binding energy per atom of the optimized monolayer phosphorene supercell (4×4) has been found high enough (3.604 eV/atom) which approves the stability of monolayer phosphorene. Its band structure calculations find direct band gap of magnitude 0.86 eV which is in close agreement with the previous study. Two differently created divacancy structures (named DV(5|8|5)-1 and DV(5|8|5)-2) consist of five-fold and eight fold rings. Calculation of formation energy predicts DV(5|8|5)-1 system more favorable to occur (formation energy = 2.743 eV) comparing to DV(5|8|5)-2 (formation energy = 5.301 eV). The band gap of former one is larger (1.01 eV) and later one is smaller (0.1 eV) comparing to pristine phosphorene. With direct type of band gap DV(5|8|5)-1 deserves further study for practical applications like in photocells, photoconductive devices, photocatalysis.

#### ACKNOWLEDGEMENTS

The authors acknowledge the University Grants Commission, Nepal, Award no. CRG-73/74-S&T-01 for partial financial support.

#### REFERENCES

[1] Novoselov, K. S., Geim, A. K., Morozov, S. V., Jiang, D., Zhang, Y., Dubonos, S. V., Grigorieva I. V. and Alexandr, A. Electric field effect in atomically thin carbon films. *Science*, **306**, 666-669 (2004).

[2] Wolf, E. L. *Applications of graphene: an overview*. Springer International Publishing (2014).

[3] Kang, S., Lee, D., Kim, J., Capasso, A., Kang, H. S., Park, J.W., Lee, C. H. and Lee, G. H. Two-dimensional semiconducting materials for electronic and optoelectronic applications: potential and challenge. *2D materials*, **7(2)**, 022003 (2020).

[4] Yang, S., Tongay, S., Li, Y., Yue, Q., Xia, J. B., Li, S. S., Li, J. and Wei, S. H. Layer-dependent electrical and optoelectronic responses of ReSe2 nanosheet transistors. *Nanoscale*, **6**, 7226-7231 (2014).

[5] Das, S., Zhang, W., Demarteau, M., Hoffmann, A., Dubey, M. and Roelofs, A. Tunable Transport Gap in Phosphorene. *Nano Letters*, **14**, 5733-5739 (2014).

[6] Qiao, J., Kong, X., Hu, X. Z., Yong, F. and Ji, W. High-mobility transport anisotropy and linear dichroism in few-layer black phosphorus. *Nature Communications*, **5**, 4475-1-7 (2014).

[7] Liu, H., Neal, A. T., Zhu, Z., Xu, X., Tomanek, D., Ye, P. D. and Lou, Z. Phosphorene: An Unexplored 2D Semiconductor with a High Hole Mobility. *ACS Nano*, **8**, 4033-4041 (2014).

[8] Shao, D. F., Lu W. J., Lv H. Y. & Sun Y. P. Electron-doped phosphorene: A potential monolayer superconductor. *Europhysics Letters*, **108(6)**, 67004-1-5 (2014).

[9] Brent, J. R., Savjani, N., Lewis, E. A., Haigh, S. J., David, J. L., and O'Brien, P. Production of few-layer phosphorene by liquid exfoliation of black phosphorus. *Chemical Communications*, **50**, 13338-13341 (2014).

[10] Nishii, T., Maruyama, Y., Inabe, T. and Shirotnani, I. Synthesis and characterization of black phosphorous interaction compounds. *Synthetic Metals*, **18**, 559-564 (1987).

[11] Bridgman, P. Two new modifications of phosphorous. *Journal of the American Chemical Society*, **36**, 1344-1363 (1914).

[12] Brown, A. and Rundqvist, S. Refinement of crystal structure of black phosphorous. *Acta Crystallographica* **19**, 684-685 (1965).

[13] Dai, J. and Zenc, X.C., Bilayer Phosphorene: Effect of Stacking Order on Bandgap and Its Potential Applications in Thin-Film Solar Cells. *Journal of Physical Chemistry Letters*, **5(7)**, 1289-1293 (2014).

[14] Banhart, F., Kotakoski, J. and Krashenninnikov, A. V. Structural Defects in Graphene. *ACS Nano*, **5(1)**, 26-41(2011).

[15] Tian, W., Li, W., Yu, W. and Liu, X. A Review on Lattice Defects in Graphene: Types, Generation, Effects and Regulation, *Micromachines*, **8**, 163-1-15 (2017).

- [16] Vergara, J. M., Flórez, E., Mora-Ramos, M. E. and Correa, J. D. Effects of single vacancy on electronic properties of blue-phosphorene nanotubes. *Materials Research Express*, **7**, 015042-1-8(2020).
- [17] Dai, X. Q., Zhao, J. H., Xie, M. H., Tang, Y. N., Li, Y. H. and Zhao, B. First-principle study of magnetism induced by vacancies in graphene. *The European Physical Journal B*, **80**, 343-349 (2011).
- [18] Zhang, Y., Gao, F., Gao, S. and He, L. Tunable magnetism of a single-carbon vacancy in graphene. *Science Bulletin*, **65(3)**, 194-200 (2020).
- [19] Tao, P., Gau, H., Yang, T. and Zhang, Z. Strain-induced magnetism in MoS<sub>2</sub> monolayer with defects. *Journal of Applied Physics*, **115**, 054305-1-5 (2014).
- [20] Zheng, H., Yang, B., Wang, D., Han, R., Du, X. and Yan, Y. Tuning magnetism of monolayer MoS<sub>2</sub> by doping vacancy and applying strain. *Applied Physics Letter*, **104**, 132403-1-5 (2014).
- [21] Sharma, P. *Study of electronic and magnetic properties of phosphorene monolayer due to interplay between vacancy and strain*, M.Sc. (Physics) Dissertation, Central Department of Physics, Tribhuvan University, Nepal (2017).
- [22] Hohenberg, P. and Kohn, W. Density functional theory (DFT). *Physical Review*, **136**, B864-B871 (1964).
- [23] Kohn, W., & Sham, L. J., Self-consistent equations including exchange and correlation effect. *Physical Review*, **140**, A1133-A1134 (1965).
- [24] Grimme, S. Semiempirical GGA-type density functional constructed with a long-range dispersion correction. *Journal of Computational Chemistry*, **27(15)**, 1787-1799 (2006).
- [25] Perdew, J. P., Burke, K., & Ernzerhof, M. Generalized gradient approximation made simple. *Physical Review Letters*, **77(18)**, 3865-3868 (1996).
- [26] Giannozzi, P., Baroni, S., Bonini, N., Calandra, M., Car, R., Cavazzoni, C., Ceresoli, D., Chiarotti, G. L., Cococcioni, M., Dabo, I., Carso, A. D., Girancoli, S., Fabris, S., Fratesi, G., Gebauer, R., Gerstmann, U., Gougoussis, C., Kokalj, A., Lazzeri, M., Martin-Samos, L., Marzari, N., Mauri, F., Mazzarello, R., Paolini, S., Pasquarello, A., Paulatto, L., Sbraccia, C., Scandolo, S., Sclauzero, G., Seitsonen, A. P., Smogunov, A., Umari, P. & Wintzovitch, R. M.. QUANTUM ESPRESSO: a modular and open-source software project for quantum simulations of materials. *Journal of physics: Condensed matter*, **21(39)**, 395502-1-19 (2009).
- [27] C., Kittel. *Introduction to Solid State Physics*, John Wiley & Sons, Inc, US, 8<sup>th</sup> ed. (2013).
- [28] Pfrommer, B. G., Cote, M., Louie, S. G. & Cohen, M. L. Relaxation of crystals with quasi-Newton method. *Journal of Computational Physics*, **131(1)**, 233-240 (1997).
- [29] Monkhorst, H. J., & Pack, J. D. Special points for Brillouin-zone integrations. *Physical Review B*, **13(12)**, 5188-5192 (1976).
- [30] Marzari, N., Vanderbilt, D., De Vita, A., & Payne, M. C. Thermal contraction and disordering of the Al(110) surface. *Physical Review Letters*, **82(16)**, 3296-3299 (1999).
- [31] Woomer, A. H., Farnsworth, T. W. , Hu, J., Wells, R. A., Donley, C. L., & Warren, S. C. Phosphorene: synthesis, scale-up, and quantitative optical spectroscopy. *ACS nano*, **9(9)**, 8869-8884 (2015).
- [32] Hu, W. & Yang, J. Defects in Phosphorene. *Journal of Physical Chemistry C*, **119**, 35, 20474-20480 (2015).
- [33] Chintalapati, S., Shen, L., Xiong, Q. & Ping Feng, Y. Magnetism in phosphorene: Interplay between vacancy and strain. *Applied Physics Letter*, **107**, 072401-1-4 (2015).